2 Interaction between atoms and a light field

In this chapter we will treat the atom–light interaction in a semiclassical way, i.e. we will adopt for the atoms a quantum–mechanical (qm) description while we use classical expressions for the light field. For this we consider atoms with two levels E_1, E_2 only (see Fig. 1) undergoing absorption and emission processes as described in Chapter 1 and following in parts the treatment of [1].

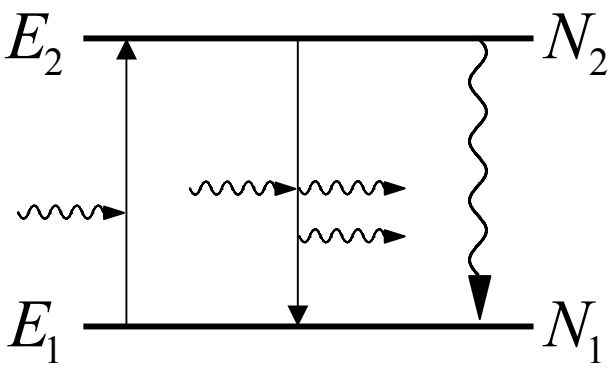

Figure 1: Resonant absorption and emission processes for a two–level atom. Left: An incident photon is absorbed and the atom is excited from the ground state E_1 to the excited state E_2. Center: An incident photon stimulates a transition, i.e. the excited state E_2 is de–excited to the ground state E_1 and a photon is created in the same mode as the incident photon. Right: An excited state decays spontaneously and emits a photon.

Rate equations

If a thermal light field with energy density $\rho(\nu)$ illuminates a two–level atom we have the rates for absorption, for induced emission and for spontaneous emission

$$\dot{N}_1 = N_1 B\rho(\nu), \qquad \dot{N}_2 = N_2 B\rho(\nu), \qquad \dot{N}_2 = N_2 A. \tag{1}$$

The Einstein A and B coefficients describe properties of the atom and do not depend on the radiation field. Thus, a simple generalization of the interaction can be obtained by generalizing the rates using a more general expression for the radiation field, as for example given by the sum of a thermal field $\rho_T(\nu)$ and an external field with a specified radiation density $\rho_E\nu$, that is we put

$$\rho(\nu) = \rho_T(\nu) + \rho_E(\nu). \tag{2}$$

Detailed balance requires $\dot{N}_2 = -\dot{N}_1$ and we obtain

$$\dot{N}_1 = N_1 A - N_1 B\rho(\nu) + N_2 B\rho(\nu). \tag{3}$$

Thus, for two–level atoms we can calculate the optical excitation as a function of the time for which we apply the incident light field. Here we consider the absorbing sample to be "optically thin", i.e. we assume that the incident light field is changed during the transmission through the sample in a negligible way. With initial conditions such that for $t = 0$ all atoms are in the ground state (i.e. $N_2(t = 0) = 0$) we obtain

$$N_2(t) = \frac{NB\rho(\nu)}{A + 2B\rho(\nu)} \left(1 - e^{-(A+2B\rho(\nu))t}\right). \tag{4}$$

The population $N_2(t)$ grows at first linearly in time and then reaches a steady state value

$$N_2^{SS} = \frac{NB\rho(\nu)}{A + 2B\rho(\nu)} \tag{5}$$

as indicated in Fig. 2.

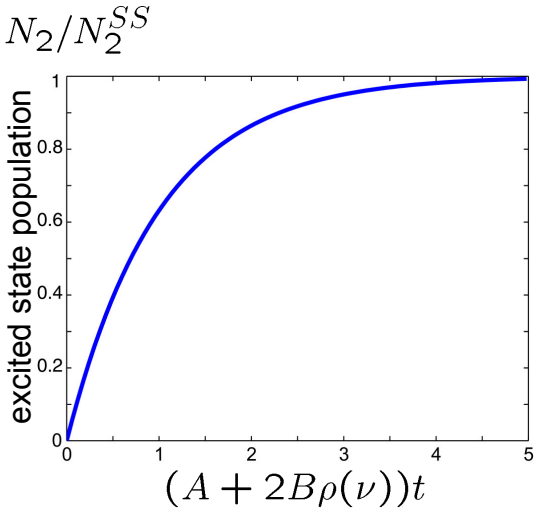

Figure 2: Relative number of excited atoms (population) as a function of the excitation time t.

Note that for thermal radiation $\rho_T(\nu) = A/B\langle n\rangle$ and with the mean photon number (see chapter 1)

$$\langle n\rangle = \frac{1}{e^{h\nu/k_BT} - 1} \tag{6}$$

present in the mode, the ratio of spontaneous and stimulated transitions at the transition frequency ν is determined by the ratio A/B. For thermal radiation at room temperature $\langle n\rangle \approx 1$ for $h\nu/k_BT \approx 0.7$ which corresponds to a radiation at a frequency of $\nu \approx 6 \times 10^{12} Hz$. Thus for an interaction with radiation of lower frequencies (infrared and microwave domain) we have (see also the discussion in [1])

$$h\nu \ll k_BT \qquad \text{and} \qquad A \ll B\rho(\nu) \tag{7}$$

whereas for radiation frequencies in the near infrared and above spontaneous emission dominates the transition rates, i.e.

$$h\nu \ll k_BT \qquad \text{and} \qquad \rho(\nu) \ll A \tag{8}$$

when thermal radiation is considered. However, with radiation present having most of its energy density at a single frequency or within a narrow bandwidth, as e.g. with a laser, induced and stimulated transition rates may greatly exceed the thermal rates.

Note: The rate equation treatment is usually sufficient to describe experiments using week excitations, i.e. excitations with mean photon number $\langle n\rangle \ll 1$ per mode which is the case for attenuated laser light or with less coherent light sources, as e.g. discharge lamps. In particular, the rate equation approach is always sufficient when the spontaneous emission rate determines the dynamic behavior

of the atomic population, e.g. when after an excitation the incident radiation is switched off. Such experiments are usually performed to measure, for example, the A coefficients as indicated in Fig. 3.

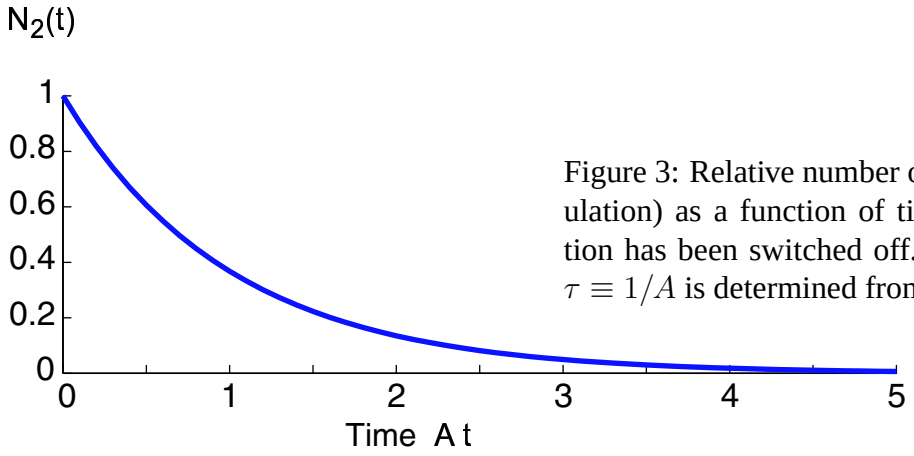

Figure 3: Relative number of excited atoms (population) as a function of time t after the excitation has been switched off. The atomic lifetime $\tau \equiv 1/A$ is determined from the decay.

2.1 Density matrix and optical Bloch equations

For a more detailed treatment of the interaction of atoms with a classical light wave we now consider the atoms as quantum mechanical two–level systems described by the wavefunction $\Psi(\vec{r},t)$ and governed by the Schrödinger equation $\hat{H}\Psi = i\hbar\partial_t\Psi$. Following the treatment in [1], we denote for the stationary Hamiltonians $\hat{H}_E$ the solutions

$$\Psi(\vec{r},t) = e^{-i\frac{E_n}{\hbar}t}\psi_n(\vec{r}), \qquad \hat{H}_E\psi_n(\vec{r}) = E_n\psi_n(\vec{r}) \tag{9}$$

which describe stationary states, in this case the eigenstates E_1, E_2. For the interaction with a light field we write the Hamiltonian

$$\hat{H} = \hat{H}_E + \hat{H}_I, \tag{10}$$

with a time dependent interaction term $\hat{H}_I = \hat{H}_I(t)$ and for a two–level system we denote

$$\Psi(\vec{r},t) = c_1(t)\Psi_1(\vec{r},t) + c_2(t)\Psi_2(\vec{r},t) \tag{11}$$

with the normalization $|c_1(t)|^2 + |c_2(t)|^2 = 1$. Inserting $\Psi(\vec{r},t)$ into the Schrödinger equation, multiplying from left with $\Psi_1^*(\vec{r},t)$ and integrating over all spatial coordinates (and likewise multiplying from the left with $\Psi_2^*(\vec{r},t)$ and integrating in the same way) yields then a set of differential equations for the amplitude coefficients $c_i(t)$ which describe the dynamical evolution of the wavefunction. After some algebra we arrive at

$$i\dot{c_1} = c_1\langle 1|\hat{H}_I|1\rangle + c_2 e^{-i\omega_0 t}\langle 1|\hat{H}_I|2\rangle \tag{12}$$

$$i\dot{c_2} = c_1 e^{i\omega_0 t}\langle 2|\hat{H}_I|1\rangle + c_2\langle 2|\hat{H}_I|2\rangle \tag{13}$$

where $\langle i|\hat{H}_I|j\rangle = \int \psi_i^*\hat{H}_I\psi_j dV$ denotes the matrix elements of the interaction Hamilitonian $\hat{H}_I$.

Interaction Hamiltonian

Consider an atom as depicted in Fig. 4 where the nucleus (charge Ze) is located at the origin of the coordinate system and the vectors $\vec{r}_i(t)$ describe the positions of the electrons with charge $-e$. The atom interacts with a polarized light field oriented as shown in Fig. 4.

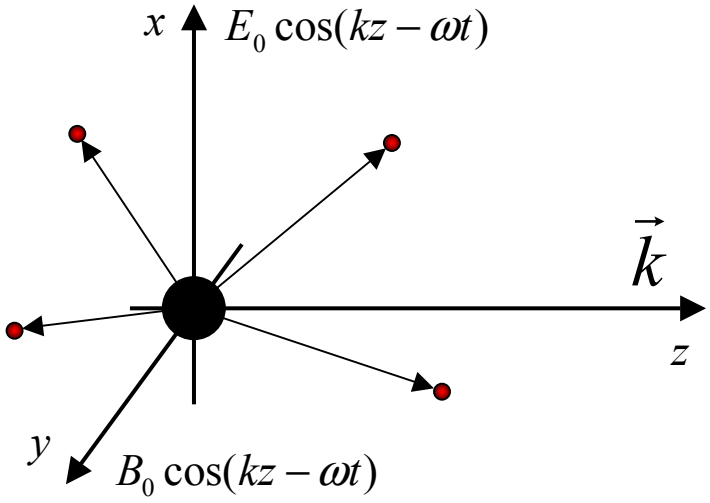

Figure 4: Coordinate system for the atom and the interacting em. wave (after [1]).

Note that $|\vec{r}_i| \ll \lambda$, i.e. the spatial extension of the $\vec{E}$ and $\vec{B}$ fields is large compared to the atoms size ($|\vec{r}| \sim a_0 = 5 \times 10^{-11}$, with the Bohr radius a_0). Therefore, $ka_0 \ll 1$ and the spatial variations of the em. wave across the atom become negligible. Thus, it is a good approximation to set $z = 0$ in the cosines indicated in Fig. 4. The total electric–dipole moment of the atom is then given by $-e\vec{D}$ where

$$\vec{D} = \sum_{j=1}^{Z} \vec{r}_j. \tag{14}$$

The interaction energy is then given by orientation of this electric–dipole moment in the electric field of the light beam and this results in the interaction Hamiltonian

$$\hat{H}_I = e\vec{D}\cos(\omega t) \tag{15}$$

which is the dipole approximation of the interaction. Higher multipole contributions are much smaller and are usually neglected in quantum optics experiments. Note that $\hat{H}_I$ is real, and it has odd parity, i.e. $\hat{H}_I$ changes sign when replacing $\vec{r}_j$ by $-\vec{r}_j$. Therefore, its diagonal matrix elements $\langle 1|\hat{H}_I|1\rangle = \langle 2|\hat{H}_I|2\rangle = 0$ (in the atomic state basis) vanish and for the off–diagonal elements we obtain

$$\langle 2|\hat{H}_I|1\rangle = \langle 1|\hat{H}_I|2\rangle^* \tag{16}$$

provided the two atomic states have opposite parity. Explicitly, since $\vec{E}_0$ points along the x-direction, these matrix elements are given by

$$\langle 1|\hat{H}_I|2\rangle = eE_0X_{12}\cos(\omega t), \qquad X_{12} = \int \psi_1^* X \psi dV \tag{17}$$

where X is the x component of the atomic dipole $\vec{D}$. For the strength of the interaction we (conventionally) write a frequency

$$\Omega = \frac{\vec{d}\vec{E}}{\hbar}, \tag{18}$$

where $\vec{d} = e\vec{X}_{12}$.

Inserting these relations into the differential equations (13), seeking an approximate solution for week excitation and comparing the result for the excited state population $|c_2(t)|^2$ with the rate equations above (i.e. the excitation $N_2(t)$ as e.g. given by rate equation result (4)) eventually results in expressions for the Einstein coefficients. The detailed derivation is given in Ref. [1] and omitted here for brevity. Explicitly, one obtains

$$B = \frac{\pi e^2 |D_{12}|^2}{3\varepsilon_0 \hbar^2} \tag{19}$$

$$A = \frac{e^2 \omega_0^3 |D_{12}|^2}{3\pi\varepsilon_0 \hbar c^3}, \tag{20}$$

with $D_{12} = eX_{12}$. These expressions are valid for a two–level system without degeneracy, otherwise statistical weights have to be included (for details see [1]).

Density matrix

The density matrix formalism is well known from quantum mechanics, here we just summarize the main features and its use for understanding and describing the experiments discussed below.

Consider a wave function

$$|\psi\rangle = \sum_n c_n(t)|u_n\rangle, \qquad \sum_n |c_n|^2 = 1 \tag{21}$$

with the orthonormal basis $\{|u_n\rangle\}$. For an observable $\hat{A}$ we write the matrix element

$$\langle u_n|\hat{A}|u_p\rangle = A_{np} \tag{22}$$

and the expectation value (at time t)

$$\langle\hat{A}\rangle(t) = \langle\psi(t)|\hat{A}|\psi(t)\rangle \tag{23}$$

$$= \sum_{n,p} c_n^*(t) c_p(t) A_{np}. \tag{24}$$

The dynamic evolution is described by the Schrödinger equation

$$i\hbar\partial_t|\psi(t)\rangle = \hat{H}(t)|\psi(t)\rangle \tag{25}$$

with the Hamilitonian $\hat{H}$. Note that the expectation values always consist of expressions $c_n^* c_p$, corresponding to matrix elements of the operator

$$|\psi(t)\rangle\langle\psi(t)| \tag{26}$$

that is, e.g. $\langle u_p|\psi(t)\rangle\langle\psi(t)|u_n\rangle = c_n^*(t)c_p(t)$. Therefore, we define the density operator (for details see books on Quantum Mechanics, e.g. [2])

$$\hat{\rho} = |\psi(t)\rangle\langle\psi(t)| \tag{27}$$

for which we have $\sum_n |c_n|^2 = \sum_n \rho_{nn} = \mathrm{Tr}\rho(t) = 1$ and for the expectation value of an observable $\hat{A}$ we obtain

$$\begin{aligned}
\langle\hat{A}\rangle &= \sum_{n,p} c_n^*(t)c_p(t)A_{n,p} \\
&= \sum_{n,p}\langle u_p|\psi(t)\rangle\langle\psi(t)|u_n\rangle\langle u_n|A|u_p\rangle \\
&= \sum_{n,p}\langle u_p|\rho(t)|u_n\rangle\langle u_n|A|u_p\rangle \\
&= \sum_{p}\langle u_p|\rho(t)A|u_p\rangle \\
&= \mathrm{Tr}\{\hat{\rho}(t)\hat{A}\}.
\end{aligned}$$

This is the property which makes the density formalism most useful: The calculation of an expectation value is just given by the trace of the density matrix times the observable under consideration. For the time evolution of the density matrix we obtain from the Schrödinger equation

$$i\hbar\dot{\hat{\rho}} = [\hat{H}, \hat{\rho}]. \tag{28}$$

Example: Consider the two–level system

$$|1\rangle = \begin{pmatrix} 1 \\ 0 \end{pmatrix}, |2\rangle = \begin{pmatrix} 0 \\ 1 \end{pmatrix}, \text{i.e.} |\psi\rangle = \begin{pmatrix} c_1 \\ c_2 \end{pmatrix} \tag{29}$$

and we obtain the density matrix simply by

$$|2\rangle = \begin{pmatrix} c_1 \\ c_2 \end{pmatrix} \begin{pmatrix} c_1^* & c_2^* \end{pmatrix} = \begin{pmatrix} |c_1|^2 & c_1c_2^* \\ c_2c_1^* & |c_2|^2 \end{pmatrix}. \tag{30}$$

To calculate the expectation value of the energy of the two–level system we take the energy operator

$$\hat{H}_E = i\hbar\partial_t = \begin{pmatrix} E_1 & 0 \\ 0 & E_2 \end{pmatrix} \tag{31}$$

and we obtain

$$\langle\hat{H}_E\rangle = \mathrm{Tr}\{\hat{\rho}\hat{H}_E\} = \mathrm{Tr}\begin{pmatrix} |c_1|^2E_1 & c_1c_2^*E_2 \\ c_2c_1^*E_1 & |c_2|^2E_2 \end{pmatrix} \tag{32}$$

and thus we conclude (which was evident to begin with) that

$$\langle\hat{H}_E\rangle = |c_1|^2E_1 + |c_2|^2E_2 \tag{33}$$

The diagonal elements ρ_{ii} of the density matrix are known as the *populations* and the off–diagonal elements ρ_{ij} are termed *coherences*.

Hamiltonian for two–level system

With these definitions we are (almost) ready to formulate the Hamiltonian for the two–level system interacting with an external (coherent) light field. The total Hamiltonian reads

$$\hat{H} = \hat{H}_E + \hat{H}_I + \hat{H}_R, \tag{34}$$

$\hat{H}_E$ is defined as in Eq. (31) and the interaction Hamiltonian is given by $\hat{H}_I = -\vec{\mu}\vec{E} \equiv e\vec{D}\vec{E}$. Using this notation, we write

$$\hat{H}_I = \begin{pmatrix} 0 & -\mu_{12}E^*(t) \\ -\mu_{21}E(t) & 0 \end{pmatrix}. \tag{35}$$

The final term $\hat{H}_R$ in Eq. (34) accounts for relaxation processes which have not been included so far. Here, we will not present a rigorous derivation, instead we will introduce this term in a more phenomenological way. For a detailed discussion of this term the reader is referred to textbooks of quantum mechanics (e.g. [2]) and to more theoretical treatments of quantum optics. For understanding and interpreting experiments it is sufficient to introduce relaxation(s) in a more heuristic (albeit quite correct) view, therefore we refer the interested reader to the literature available [3].

From the experimental point of view it is immediately clear that relaxation phenomena must be taken into account. First and foremost, spontaneous emission has not yet been taken into account although this seemed to be an easy task with rate equations. Moreover, any other coupling of the two–level atom with the environment (e.g. by colliding with surrounding walls or with other atoms) during its coherent interaction with the light field will lead to a perturbation of the coherent dynamics, as e.g. described by Eqs. (13). Thus, we simply have to take into account (as for the rate equations) that spontaneous emission and possibly other perturbing effects cause the excited state population to decay to the ground state. Therefore, we phenomenologically include a decay rate

$$|2\rangle \xrightarrow{\Gamma} |1\rangle \tag{36}$$

and define this in terms of matrix elements of the "relaxation term" $\hat{H}_R$

$$(i\hbar)^{-1}[\hat{H}_R, \hat{\rho}]_{22} = -\rho_{22}/T_2 = -\Gamma\rho_{22} \tag{37}$$

$$(i\hbar)^{-1}[\hat{H}_R, \hat{\rho}]_{11} = \rho_{22}/T_2 = (1-\rho_{22})\Gamma \tag{38}$$

where we have introduced the lifetime $T_2 = 1/\Gamma$ of the excited state $|2\rangle$. In this way, we account for any population changes of state $|2\rangle$ which, of course, can only end up to refill state $|1\rangle$. Such relaxations are known from NMR (nuclear magnetic resonance) and ESR (electron spin resonance) techniques and are here included in the same way. The corresponding relaxation time T_2 is due to a population change and is called (by convention from NMR and ESR) the "longitudinal relaxation".

State $|1\rangle$ was assumed to be the ground state and thus to be stable (i.e. we do not include any population changes from $|1\rangle \rightarrow |2\rangle$, for example, by collisions which would only be possible if there were enough energy available). Thus a relaxation time T_1 which is more generally considered in NMR and ESR is not included here, or more precisely, we take $T_1 \rightarrow \infty$.

As can be already inferred from the differential equations (13) and likewise from the density matrix formalism the populations are inherently coupled by the Schrödinger equation to the coherences and therefore relaxation has to be taken into account for the coherences as well. For the two–level system and the interaction present there are two off–diagonal terms for which we write

$$(i\hbar)^{-1}[\hat{H}_R, \hat{\rho}]_{12} = -\rho_{12}/T_{21} = -\gamma\rho_{12} \tag{39}$$
$$(i\hbar)^{-1}[\hat{H}_R, \hat{\rho}]_{11} = -\rho_{21}/T_{21} = -\gamma\rho_{21}. \tag{40}$$

This relaxation is known as the "transverse relaxation" with the relaxation time $T_{21} = T_{12}$ and the rate $\gamma = T_{21}^{-1}$. The transverse relaxation is linked to the longitudinal relaxation in the following way

$$T_{21}^{-1} = \gamma = \frac{1}{2}(T_1^{-1} + T_2^{-1}) + \gamma_\phi \tag{41}$$

where the rate γ_ϕ describes the rate of events which perturb the phase relationship between the exciting field and the coherently driven atom. Thus, collisions (with a surrounding wall or other atoms) can be taken into account. The rate γ_ϕ is therefore known as the "dephasing" rate and since it is mostly due to collisions, it is often referred to as collision rate. Note however, that a finite bandwidth of the exciting frequency (for example resulting from frequency fluctuations of a laser) can be added here to properly account for phase decoherence.

For well prepared systems in quantum optics experiments, the lifetime of the ground state (i.e. T_1) needs not to be considered (i.e. $T_1 \rightarrow \infty$) and the dephasing rate is set to zero. Thus, for many experiments in quantum optics, one is able to reduce this treatment to the case of pure *radiation damping* which is determined by the relation

$$\gamma = \frac{1}{2}\Gamma. \tag{42}$$

In summary, we obtain

$$[\hat{H}_R, \hat{\rho}] = i\hbar \begin{pmatrix} \Gamma\rho_{22} & -\gamma\rho 12 \\ -\gamma\rho_{21} & -\Gamma\rho_{22} \end{pmatrix}. \tag{43}$$

and we write

$$\hat{H} = \underbrace{\hat{H}_E + \hat{H}_I}_{} + \hat{H}_R = \hat{H}_W + \hat{H}_R \tag{44}$$

such that we obtain

$$i\hbar\dot{\hat{\rho}} = [\hat{H}, \hat{\rho}] = [\hat{H}_W, \hat{\rho}] + [\hat{H}_R, \hat{\rho}] \tag{45}$$

with

$$\hat{H}_W = \begin{pmatrix} E_1 & -\frac{\mu E}{2}(e^{i\omega t}+e^{-i\omega t}) \\ -\frac{\mu E}{2}(e^{i\omega t}+e^{-i\omega t}) & E_2 \end{pmatrix} \quad \text{and} \quad \hat{\rho} = \begin{pmatrix} \rho_{11} & \rho_{12} \\ \rho_{21} & \rho_{22} \end{pmatrix}. \tag{46}$$

The electric field is considered to be real, i.e. $E = E^*$ and we use $\cos\omega t = \frac{1}{2}(e^{i\omega t}+e^{-i\omega t})$.

Using these notations, and inserting this in the Heisenberg equation (28), we obtain after some algebra the following equations for the two–level system interacting with the radiation field E

$$\begin{aligned}
i\hbar\dot{\rho_{11}} &= \frac{\mu E}{2}(e^{i\omega t}+e^{-i\omega t})(\rho_{21}-\rho_{12}) + i\hbar\Gamma\rho_{22} && (47)\\
i\hbar\dot{\rho_{12}} &= \rho_{12}(E_1-E_2) - \frac{\mu E}{2}(e^{i\omega t}+e^{-i\omega t})(\rho_{11}-\rho_{22}) - i\hbar\gamma\rho_{12} && (48)\\
i\hbar\dot{\rho_{21}} &= -\frac{\mu E}{2}(e^{i\omega t}+e^{-i\omega t})(\rho_{11}-\rho_{22}) + \rho_{21}(E_2-E_1) - i\hbar\gamma\rho_{21} && (49)\\
i\hbar\dot{\rho_{22}} &= \frac{\mu E}{2}(e^{i\omega t}+e^{-i\omega t})(\rho_{21}-\rho_{12}) - i\hbar\Gamma\rho_{22} && (50)
\end{aligned}$$

Note that $\dot{\rho_{11}} = -\dot{\rho_{22}}$ and $\dot{\rho^*_{12}} = \dot{\rho_{21}}$. We denote for the frequency difference $\omega_{ij} = (E_i - E_j)/\hbar$, introduce the detuning $\Delta = \omega_{21} - \omega$ and we adopt the notation $\Omega = \mu E/\hbar$. Then these equations are transformed to a rotating frame, i.e. we introduce the slowly varying coherences $\tilde{\rho_{12}}$ and $\tilde{\rho_{21}}$ by setting

$$\rho_{12} = \tilde{\rho_{12}}e^{i\omega t}, \rho_{21} = \tilde{\rho_{21}}e^{-i\omega t} \tag{51}$$

and then we obtain after neglecting terms which rotate with twice the optical frequency (rotating wave approximation) the so–called optical Bloch equations for the two–level system

$$\begin{aligned}
\dot{\rho}_{11} &= \frac{i\Omega}{2}(\tilde{\rho_{12}} - \tilde{\rho_{21}}) + \Gamma\rho_{22} && (52)\\
\dot{\tilde{\rho}}_{12} &= \frac{i\Omega}{2}(\rho_{11}-\rho_{22}) + (i\Delta - \gamma)\tilde{\rho_{12}} && (53)\\
\dot{\tilde{\rho}}_{21} &= -\frac{i\Omega}{2}(\rho_{11}-\rho_{22}) - (i\Delta + \gamma)\tilde{\rho_{21}} && (54)\\
\dot{\rho}_{22} &= -\frac{i\Omega}{2}(\tilde{\rho_{12}} - \tilde{\rho_{21}}) - \Gamma\rho_{22}. && (55)
\end{aligned}$$

These equations (52–55) (in a rotating frame and using the RWA) describe the dynamic behavior of a two–level system interacting with a coherent light field and include relaxation processes in a phenomenological way. Note that we have properly denoted all slowly varying elements by adding the ~ to the coherences. In the literature, the tildes are most often omitted, as we will do below as well. However, always keep in mind that the coherences are to be understood in a rotating frame and that they must be properly transformed back to the laboratory frame.

2.2 Rabi oscillations

For a solution of the optical Bloch equations (OBE (52–55)) we make the ansatz

$$\rho_{ij} = \rho_{ij}^{(0)} e^{\lambda t} \tag{56}$$

and we drop the tildes from now on. Inserting eq. (56) into the OBE then yields the system of equations

$$\begin{pmatrix} -\lambda & \frac{i\Omega}{2} & -\frac{i\Omega}{2} & \Gamma \\ \frac{i\Omega}{2} & i\Delta - \gamma - \lambda & 0 & -\frac{i\Omega}{2} \\ -\frac{i\Omega}{2} & 0 & -i\Delta - \gamma - \lambda & \frac{i\Omega}{2} \\ 0 & -\frac{i\Omega}{2} & \frac{i\Omega}{2} & -\Gamma - \lambda \end{pmatrix} \begin{pmatrix} \rho_{11}^0 \\ \rho_{12}^0 \\ \rho_{21}^0 \\ \rho_{22}^0 \end{pmatrix} = 0 \tag{57}$$

and we consider this at first without damping, i.e. we set $\Gamma = \gamma = 0$. For the eigenvalues λ we obtain

$$\lambda^2(\lambda^2 + \Delta^2 + \Omega^2) = 0 \tag{58}$$

which yields the roots $\lambda_1 = 0$ (twofold) and $\lambda_2 = i\Omega'$, $\lambda_3 = -i\Omega'$ where we define $\Omega' = (\Delta^2 + \Omega^2)^{1/2}$. Thus the solution of the OBE can be written as

$$\rho_{ij} = \rho_{ij}^{(1)} + \rho_{ij}^{(2)} e^{i\Omega t} + \rho_{ij}^{(3)} e^{-i\Omega t} \tag{59}$$

and we obtain (see [1] for details) with the initial conditions $\rho_{22}(t=0) = 0$ and $\rho_{12}(t=0) = 0$ the solutions

$$\rho_{22} = \frac{\Omega^2}{\Omega'^2} \sin^2 \frac{\Omega' t}{2} \tag{60}$$

$$\rho_{12} = e^{i\Delta t} \frac{\Omega^2}{\Omega'^2} \sin \frac{\Omega' t}{2} \left(\Delta \sin \frac{\Omega' t}{2} + i\Omega \cos \frac{\Omega' t}{2} \right). \tag{61}$$

Fig. 5 shows the solutions (61) for different ratios of the detuning $\omega_0 - \omega$ to the interaction strength Ω which is called the *Rabi–frequency*. For $\Delta/\Omega = 0$ the solutions show full modulation, i.e. the population changes sinusoidally between the excited state $\rho_{22} = 1$ and the ground state $\rho_{22} = 1 - \rho_{11} = 0$ with frequency Ω (so–called *Rabi–oscillations* or *Rabi–flopping*. For larger detunings the frequency gets larger (according to $\Omega' = (\Delta^2 + \Omega^2)^{1/2}$, the so–called generalized Rabi–frequency) and the population in the excited state gets smaller because of the non–resonant excitation.

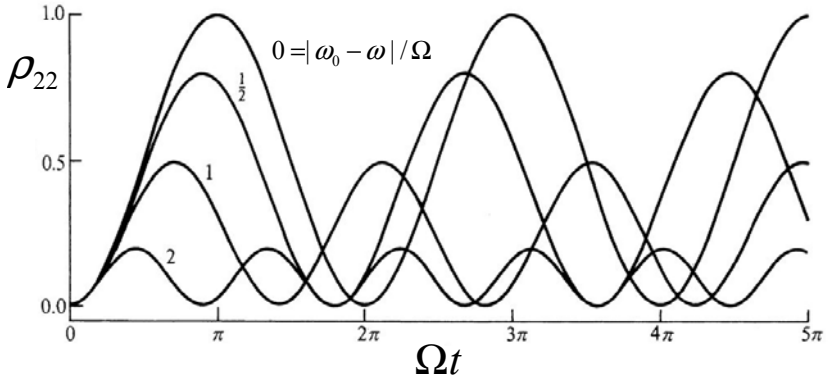

Figure 5: Excited state population for different ratios of the detuning Δ to the Rabi–frequency Ω (from [1]).

Influence of damping

When damping is included (i.e. $\Gamma, \gamma \neq 0$), then it is no longer possible to give the general solution of the OBE in an explicit and simple analytic form. Therefore (and following the treatment in [1]) we consider two limiting cases: i) $\omega = \omega_0$ (resonance) and ii) $\Omega \ll \gamma$ (weak excitation).

Resonant excitation ($\omega = \omega_0$): One obtains

$$\rho_{22}(t) = \frac{\frac{1}{2}\,\Omega^2}{2\gamma^2 + \Omega^2}\left[1 - \left(\cos\lambda t + \frac{3\gamma}{2\lambda}\sin\lambda t\right) e^{-\frac{3\gamma t}{2}}\right] \tag{62}$$

where we have defined $\lambda = [\Omega^2 - 1/4\gamma^2)^{1/2}$ with the usual initial conditions $\rho_{22}(t = 0) = 0$ and $\rho_{12}(t = 0) = 0$. Fig. 6 shows these solutions with different ratios of γ/Ω. Even for non–zero damping Rabi–flopping remains visible though increasingly damped. Experimental observation of an oscillatory behavior is always considered to indicate a coherent atom–radiation interaction, in case it is damped, the coherent interaction time is limited to the time during which oscillations can be observed.

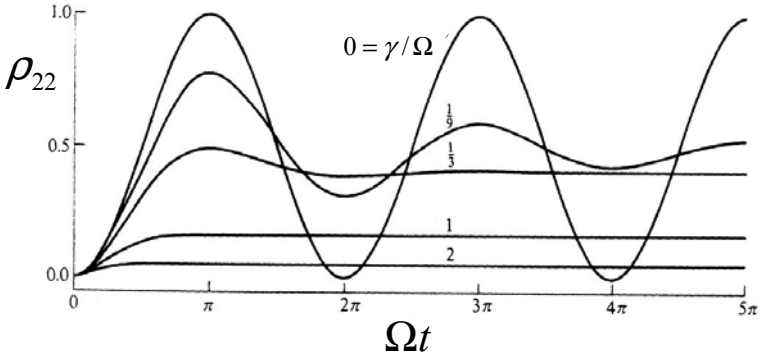

Figure 6: Resonant excitation ($\omega = \omega_0$): Excited state population for different ratios of the damping γ to the Rabi–frequency Ω (from [1]).

Weak excitation ($\Omega \ll \gamma$): One obtains

$$\rho_{22}(t) = \frac{\frac{1}{4}\,\Omega^2}{2\Delta^2 + \gamma^2}\left(1 + e^{-2\gamma t} - 2\cos\Delta t e^{-\gamma t}\right) \tag{63}$$

for initial conditions $\rho_{22}(t = 0) = 0$ and $\rho_{12}(t = 0) = 0$. Fig. 7 shows these solutions with different ratios of Δ/γ. Note that in this case the vertical axis has been re–scaled and $\rho_{22}(t) \ll 1$ because of $\Omega \ll \gamma$. For off-resonant detuning an oscillatory behavior with very small amplitudes can still be observed.

For spectroscopic investigations one is usually interested in the excited state population as a function of the detuning which in turn is usually measured as a steady state value. Therefore, we are interested in (steady state) solutions, i.e. for measurement times $T \to \infty$ or at least $T \gg 1/\Gamma$, and thus we require $\dot{\rho}_{ij} = 0$ and solve for $\rho = \rho(\Delta)$. This yields

$$\rho_{22}^{SS} = \frac{\Omega^2/4}{\Delta^2 + \gamma^2 + \Omega^2/2} \tag{64}$$

$$\rho_{12}^{SS} = e^{i\Delta t}\frac{\Omega/2(\Delta + i\gamma)}{\Delta^2 + \gamma^2 + \Omega^2/2}, \tag{65}$$

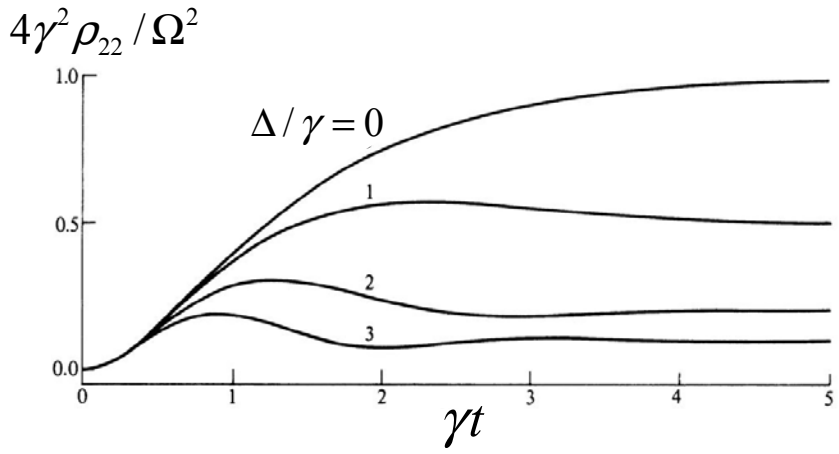

Figure 7: Weak excitation ($\Omega \ll \gamma$): Excited state population for different ratios of the detuning Δ to the damping γ (from [1]).

where eq. (64) denotes the *Lorentzian* absorption profile and eq. (65) is the dispersion profile that indicates the index of refraction. For pure radiation damping ($\gamma = 1/2\,\Gamma$) the FWHM of the Lorentz–profile is $2\gamma = \Gamma$. Note that the denominator of eq.(64) contains an Ω^2 term, i.e. the observed linewidth depends on the incident intensity and thus this term can cause the so–called *power broadening*. In the presence of elastic (phase changing) collisions the linewidth may be determined by the dephasing rate or the collision rate. This results in a collision broadening of the spectral line. Both, power broadening and collision broadening are affecting the contributing atoms in the same way and thus result in a *homogeneous* broadening.

This is different when the contributing shifts and broadenings are different for the contributing atoms, as e.g., is the case for the Doppler–shift $\omega = \omega_0(1 \pm v/c)$. As a result from the velocity distribution (for example a Maxwell distribution for velocities v_z along an axis z: $dN/dv_z = \exp(-m/2\,v_z^2/kT)$) different velocities give different resonance frequencies for an ensemble of atoms and thus this leads to an *inhomogeneous* broadening of the spectral line. A Doppler–broadened line acquires a Gaussian lineshape with a FWHM of

$$2\Delta^D = 2\omega_0 \left(\frac{2kT}{mc^2}\ln 2\right)^{1/2} \tag{66}$$

when $\Delta^D \gg \Gamma, \gamma$ and if Δ^D is comparable with γ, Γ, the lineshape must be obtained by a convolution of the atomic Lorentzian and the Gaussian profile due to the velocity distribution (i.e. it acquires a *Voigt*–profile).

2.3 Vector model of the density matrix

The interaction of a two–level system with a coherent light field has been described above using the density matrix approach and we derived the optical Bloch equations (OBGs, eqs. (52–55)) which describe the dynamical behavior of the populations and the coherences. Historically, an electron spin in a constant magnetic field (which constitutes a two–level system) interacting with a transverse time–dependent magnetic field was described already in the 1940s by F. Bloch and represents the basis for all ESR and NMR experiments until today. This treatment was shown to be completely equivalent with the density matrix approach by R. P. Feynman, F. L. Vernon and R. W. Hellwarth [4] valid for any two–level system and hence the name *optical Bloch equations* for the describing formulae.

In agreement to the treatment of a spin we define the components of the so–called *Bloch–vector* as

$$\begin{aligned} U &= \rho_{21}e^{i\omega t} + \rho_{12}e^{-i\omega t} \\ V &= i(\rho_{21}e^{i\omega t} - \rho_{12}e^{-i\omega t}) \\ W &= \rho_{22} - \rho_{11} \end{aligned} \tag{67}$$

and we obtain

$$\begin{aligned} \rho_{21} &= \frac{1}{2}(U - iV)e^{-i\omega t} \\ \rho_{12} &= \frac{1}{2}(U + iV)e^{i\omega t}. \end{aligned} \tag{68}$$

Note that U, V, W are slowly varying on the time scale of the transition frequency. The components are written in vectorial form as

$$\vec{U} = U\vec{e_x}\sigma_x + V\vec{e_y}\sigma_y + W\vec{e_z}\sigma_z = \mathrm{Tr}(\rho'\vec{\sigma}) \tag{69}$$

with the Pauli spin tensor

$$\vec{\sigma} = \vec{e_x}\sigma_x + \vec{e_y}\sigma_y + \vec{e_z}\sigma_z \tag{70}$$

and with ρ' being a representation of the density matrix in the interaction picture, i.e.

$$\rho' = \begin{pmatrix} \rho_{22} & \rho_{21}e^{i\omega t} \\ \rho_{21}e^{-i\omega t} & \rho_{11} \end{pmatrix}. \tag{71}$$

Pauli matrices and some notations: The Pauli matrices are given by

$$\sigma_x = \begin{pmatrix} 0 & 1 \\ 1 & 0 \end{pmatrix}, \sigma_y = \begin{pmatrix} 0 & -i \\ i & 0 \end{pmatrix}, \sigma_z = \begin{pmatrix} 1 & 0 \\ 0 & -1 \end{pmatrix} \tag{72}$$

and we have the *spin flip operators*

$$\sigma_- = \begin{pmatrix} 0 & 0 \\ 1 & 0 \end{pmatrix}, \sigma_+ = \begin{pmatrix} 0 & 1 \\ 0 & 0 \end{pmatrix} \tag{73}$$

which yield, for example

$$\sigma_x = \begin{pmatrix} 0 & 1 \\ 1 & 0 \end{pmatrix}\begin{pmatrix} 1 \\ 0 \end{pmatrix} = \begin{pmatrix} 0 \\ 1 \end{pmatrix}. \tag{74}$$

With $\rho'\vec{\sigma} = \rho'\vec{e_x}\sigma_x + \rho'\vec{e_y}\sigma_y + \rho'\vec{e_z}\sigma_z$ (where $\rho', \vec{\sigma}$ are defined as above (eqs. (71, 70))) we obtain, for example,

$$\rho'\sigma_x = \begin{pmatrix} \rho_{22} & \rho_{21}e^{i\omega t} \\ \rho_{21}e^{-i\omega t} & \rho_{11} \end{pmatrix}\begin{pmatrix} 0 & 1 \\ 1 & 0 \end{pmatrix} = \begin{pmatrix} \rho_{21}e^{i\omega t} & * \\ * & \rho_{21}e^{-i\omega t} \end{pmatrix} \tag{75}$$

and thus we have

$$\mathrm{Tr}(\rho'\sigma_x) = U, \mathrm{Tr}(\rho'\sigma_y) = V, \mathrm{Tr}(\rho'\sigma_z) = W \tag{76}$$

With that we can write the Bloch–equations in the following form:

$$\begin{aligned} \dot{U} &= -\Delta V - \gamma U \\ \dot{V} &= \Delta U - \gamma V + \Omega W \\ \dot{W} &= -\Gamma(W+1) - \Omega V \end{aligned} \tag{77}$$

where γ, Γ denote the decay of the coherences and populations, respectively. As for the density matrix approach we denote for the case of pure radiation damping $\gamma = \frac{1}{2}\Gamma$ and more generally, we have as before $\gamma = 1/T_2, \Gamma = 1/T_1$ and the effect of collisions can be included by denoting γ' which includes a collision rate. In summary, we therefore write

$$\dot{\vec{U}} = -\gamma'(\vec{U} + \vec{e_z}) + \vec{U} \times \vec{\Omega} \tag{78}$$

where $\vec{\Omega} = \Omega\vec{e_x} - \Delta\vec{e_z}$, which is the same form for an electron in a static magnetic field and interacting with a transverse coherent rf–field. $\vec{U}$ is called the *Bloch–vector* and $\vec{\Omega} = (\Omega, 0, \Delta)$ represents the *effective field vector*.

The eqs. (78) describe the dynamical behavior of an electron spin in a constant magnetic field $\vec{H}_0 = (0, 0, H_z^0)$ interacting with a transverse magnetic field $\vec{H}_S(t) = (H_x^S(t), H_y^S(t), 0)$ as indicated in Fig. 8.

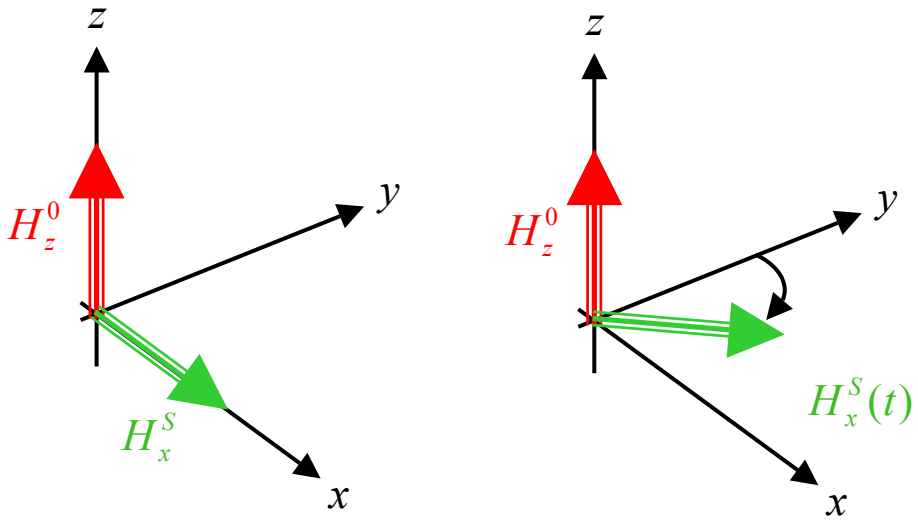

Figure 8: Configuration of the constant magnetic field H_z^0 and the transverse time-dependent field $H_x^S(t)$. The Bloch equations describe the position of the Bloch–vector under the influence of the time–dependent field $H_x^S(t)$.

Solutions of the Bloch equations

Consider for simplicity the case $\gamma = 0$ and the initial conditions $U(0) = V(0) = 0, W(0) = 1$, i.e. we consider the system to be in the ground state with no initial coherences excited. With this, one obtains [5]

$$\begin{aligned} U(t) &= \frac{\Omega\Delta}{\Omega'^2} W(0)(\cos\Omega t - 1) \\ V(t) &= \frac{\Omega}{\Omega'} W(0) \sin\Omega t \\ W(t) &= W(0)(1 + \frac{\Omega^2}{\Omega'^2}(\cos\Omega t - 1)) \end{aligned} \tag{79}$$

where $\Omega'^2 = \Omega^2 + \Delta^2$ and we denote either the expectation values of the electron spin, i.e. $\langle s_x \rangle, \langle s_y \rangle, \langle s_z \rangle$ or, equivalently (in the configuration space) the components U, V, W. These solutions are indicated in Fig. 9 and the motion of the Bloch–vector on the *Bloch–sphere* is shown in Fig. 10.

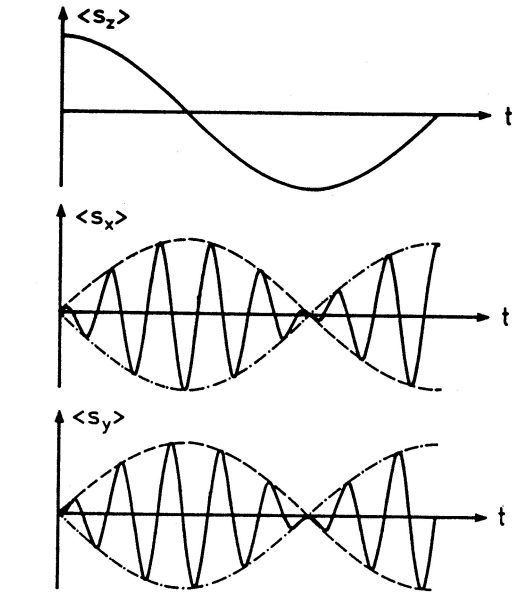

Figure 9: Expectations values of the x, y, z–components of the electron spin in a constant magnetic field and interacting with at resonant transverse time–dependent field (from [6]).

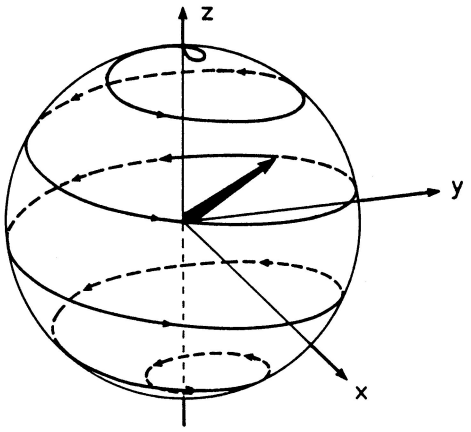

Figure 10: Motion of electron spin on the Bloch–sphere. While the the spin precesses, it spirals down, i.e. it "flips". The trace shown is the tip of the Bloch-vector (from [6]).

Whenever the Bloch–vector (or equivalently, the spin for an electron) points exactly in the $x-y$ plane, the coherences are maximally excited, i.e. we obtain $W(t) = 0$ and from eqs. (79) we conclude that this is the case for $\Delta = 0$ and $\cos \Omega t = 0$, i.e. for the condition

$$\Omega t = \frac{\pi}{2}. \tag{80}$$

Thus, for an interaction time $t = \pi/(2\Omega)$ and starting with the Bloch–vector initially pointing up (or down) the Bloch-vector moves into the *coherence plane* and accordingly such a pulse of interaction is called a $\pi/2$-pulse. Analogously, for $\Omega t = \pi$, the application of a π-pulse flips the spin by 180° (see Fig. 11).

Since the motion of a spin in a magnetic field presents a clear picture of the interaction, the terminology is similarly used when dealing with optical Bloch equations and when everything is considered in a more general Hilbert space instead of the real space. Therefore, sometimes for a two–level atom the term "Pseudo–spin" is used for the Bloch vector. For a further discussion of the analogy between the

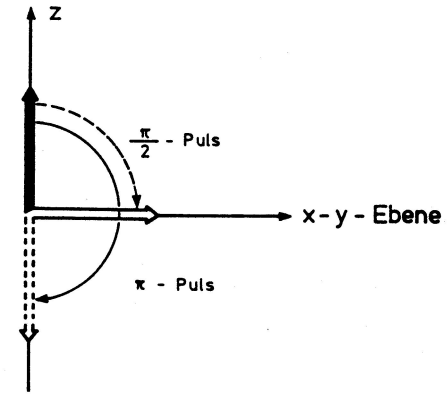

Figure 11: Application of a $\pi/2$–pulse rotates the Bloch–vector by 45°, with a π–pulse the Blochh–vector can be flipped (rotation by 180°) (from [6]).

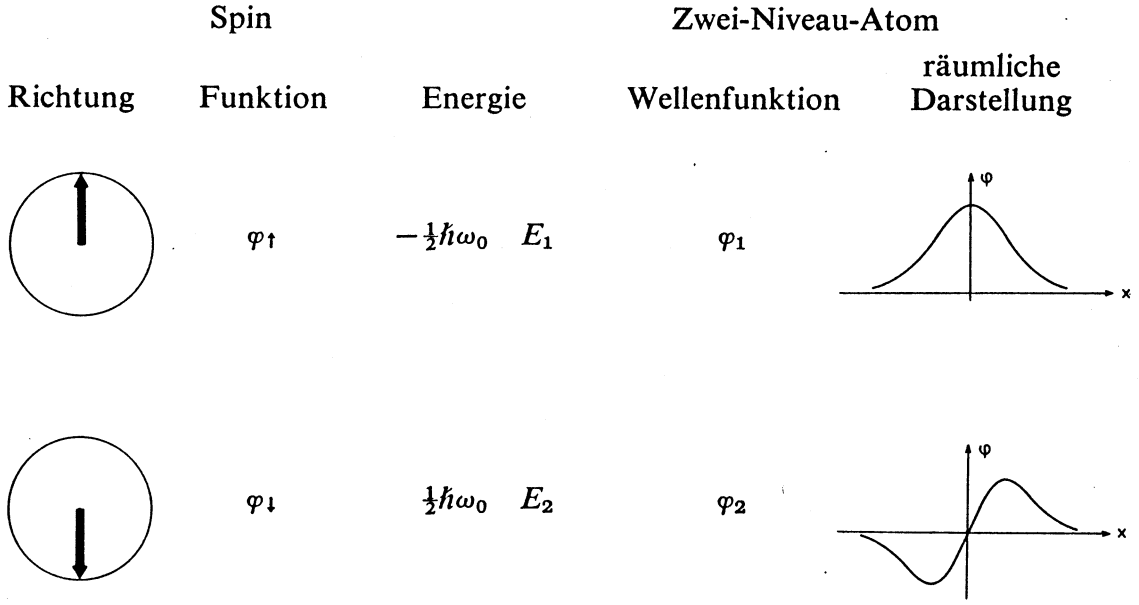

Figure 12: Analogy between spin and two–level atom: analogy between the time–dependent wave functions and the energies (from [6]).

spin of an electron and the two–level atom we refer the reader to reference [6], a summary is shown in Figs. 12, 13, 14.

Note that this vector model can be generalized in principle to a more-level system. For example, in the literature one can find a Bloch–vector description of three–level systems. However, the motion of an eight–component vector does not present a clearer picture than the density matrix formalism which is therefore the preferred choice for almost all multi–level calculations in quantum optics.

Experimental observation of Bloch vector dynamics

The dynamical behavior of the Bloch vector can be observed in a number of experiments. One of the early key experiments was performed by R. G. Brewer and R. L. Shoemaker [7]. In this experiment the ensemble of two–level atoms is provided by CH_3F–molecules (methyl fluoride) which exhibit a first–order Stark effect. Thus, the level splitting of the considered two–level system can be influenced simply by the application of an electric field and therefore the atoms can be "switched into resonance" with an exciting laser field. In this way, the interaction time t can be precisely determined

Spin

$\varphi = c_1\varphi_\downarrow + c_2\varphi_\uparrow$

freie Präzession des Spins

$c_1 = a\exp[i\omega_0 t/2]$

$c_2 = b\exp[-i\omega_0 t/2]$

Zwei-Niveau Atom (Elektron)

$\psi(\mathbf{r}) = c_1\varphi_1 + c_2\varphi_2$

freie Oszillation des Dipolmoments

$c_1 = a\exp[-iE_1 t/\hbar]$

$c_2 = b\exp[-iE_2 t/\hbar]$

Figure 13: Analogy between spin and two–level atom: wave packets without external time dependent field (from [6]).

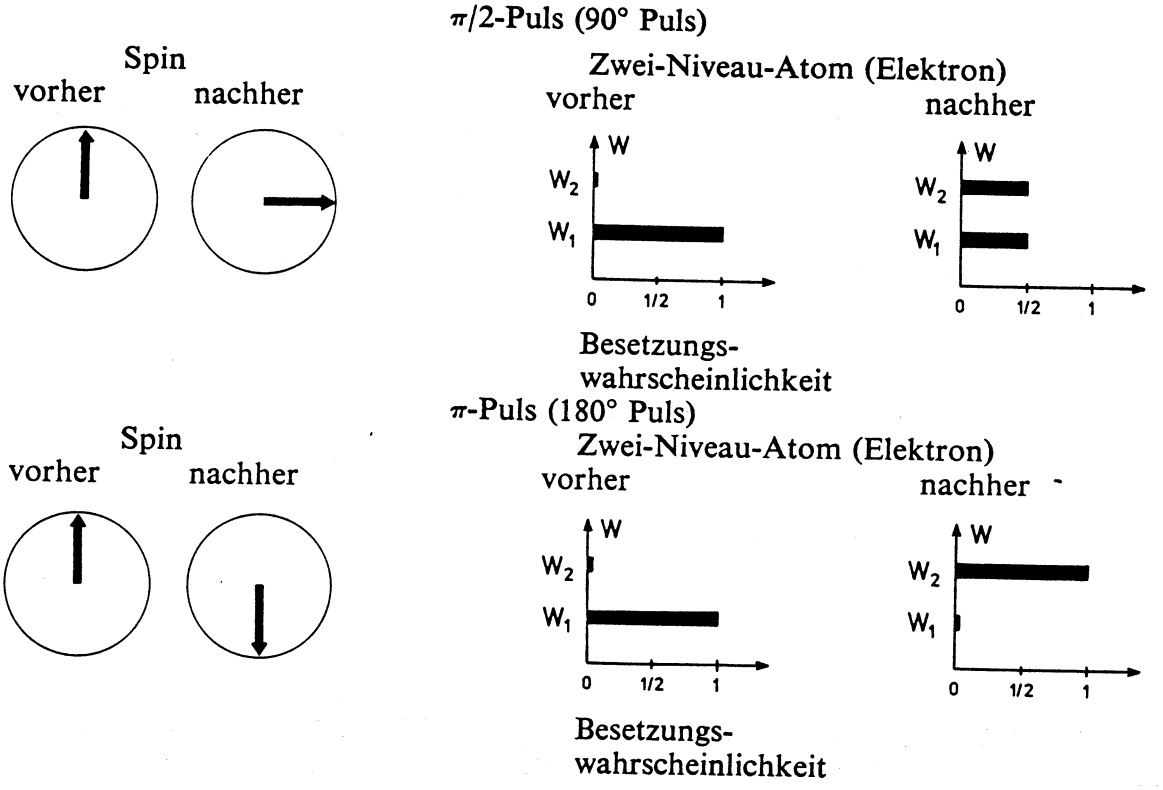

Figure 14: Analogy between spin and two–level atom: behavior of spin and two–level atom interacting with a coherent resonant field (from [6]).

as introduced in the discussion above. Transient optical signals are the observed in transmission by electronically gating the optical absorption with the pulsed electric field. The experimental scheme is indicated in Fig. 15.

The exciting wavelength is derived from a CO_2–laser which radiates near 10.6 μm and is fixed in frequency. The two–level transition of the molecules in the absorption cell has a Doppler width which exceeds the Stark shift caused by the electric field. Thus, appreciable absorption is observed even without an electric field and the detector measures a steady state intensity while the laser causes Rabi–flopping with the resonant molecules and the transitions produce oscillating macroscopic dipole moments. Immediately after switching the electric field, the resonance is shifted and absorption appears with molecules of a different velocity group. The Stark–shifted macroscopic dipole moments radiate at a different frequency which interferes with the exciting laser radiation and causes a "beat" signal at the detector which can be observed as low–frequency modulation of the detector current. Thus the nutating dipole Bloch vector can be observed as a modulation of the detector current and

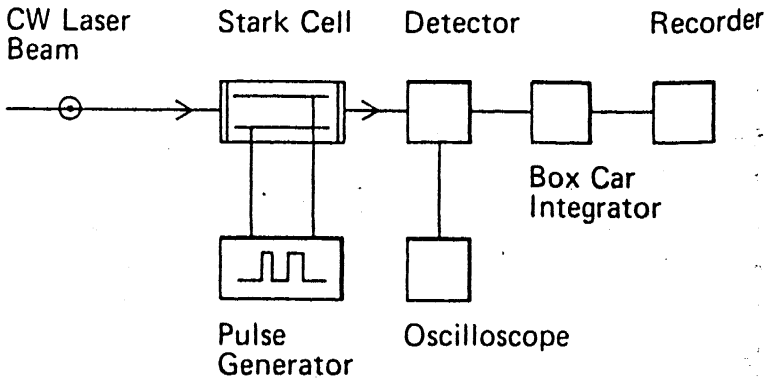

Figure 15: Level–switching technique for monitoring optical transient signals using one or more Stark pulses (from [7]).

the decay of the oscillations gives information about the T_1 and T_2 times which can be varied, for example, by changing the pressure in the Stark cell. Fig. 16 shows the resulting optical nutation signals obtained in the measurement by Brewer and Shoemaker [7].

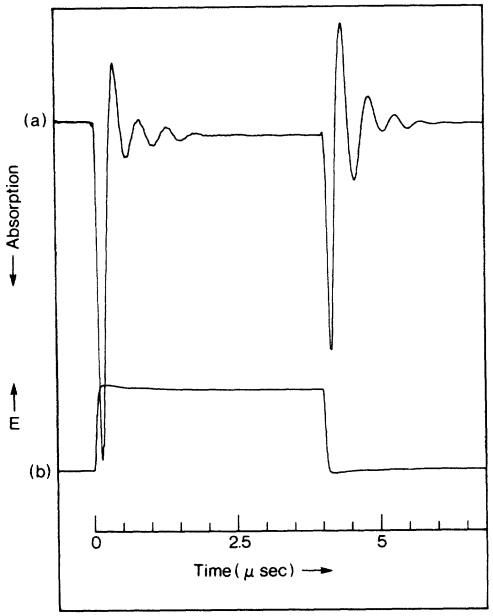

Figure 16: Damped optical nutation oscillations (a) observed by Stark–field (b)switching (from [7]).

This beautiful experimental technique was used as well for a demonstration of another optical analogue to the coherent interaction of a radiation field with an ensemble of electron spins. For this, we consider an ensemble of two–level atoms which are excited with a $\pi/2$ pulse such that the Bloch vectors of the individual excited atoms (molecules) rotate in the $x - -y$ plane, i.e. coherence is produced. As outlined above, in an ensemble of atoms there is a velocity distribution and thus the individual transition frequencies are slightly different. Therefore, the free precession of the Bloch vector of the individual atoms occurs with slightly different frequencies (due to the Doppler effect) and the macroscopic dipole moment which was, for example, produced by an initial pulse of interaction, gradually decays. This is a dephasing mechanism as introduced above. The same effects appears with spins of electrons in an ESR experiment or spins of nucleui in an NMR setup. This scenario is indicated in Fig. 17. If, after a certain time T of free precession, a π–pulse is applied to the sample, all spins are rotated by 180° (i.e. they are flipped) and they continue to precess, albeit in opposite direction. Therefore, after another free precession period of T all spins realign to form a macroscopic dipole moment because all individual phase lags or phase advances are compensated. Thus, the macroscopic dipole moment of the sample can radiate and produces an observable signal which

is called "spin–echo" with spins and accordingly termed "photon–echo" when dealing with optically excited two–level atoms.

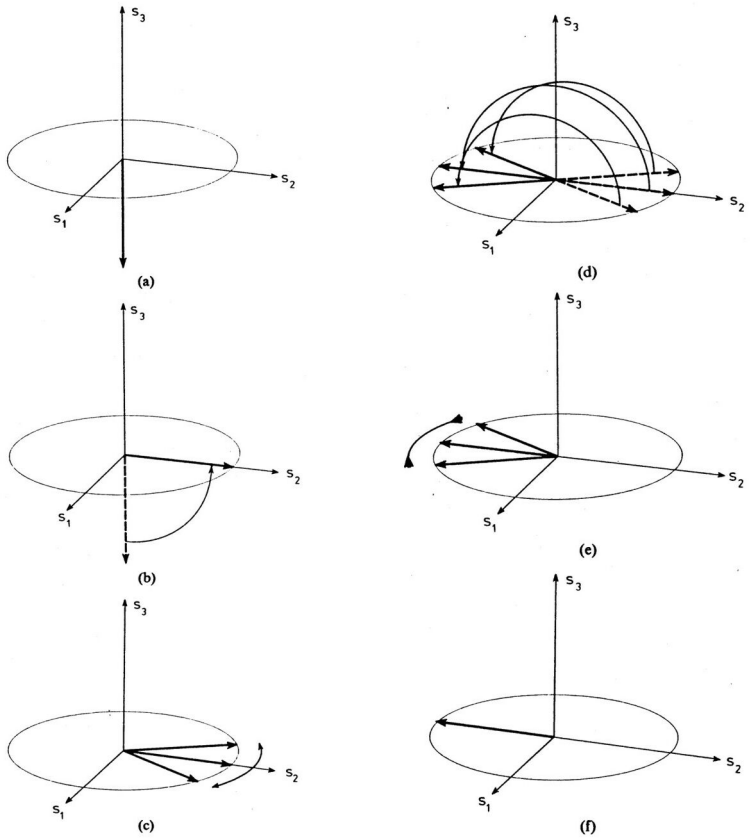

Figure 17: Dephasing spins in the rotating frame: At time $t = 0$ the spins (two–level systems) are considered to be in the ground state (a). After application of a $\pi/2$–pulse, the spins are rotated into the coherence plane and start to precess about the $z = s_3$–axis (without an external field). Since each spin precesses at its own frequency, dephasing sets in and the sample exhibits inhomogenous broadening. After a freee precession period T a π–pulse is applied to the ensemble of two–level systems and all spins (individual Bloch vectors) are rotated by 180° (d). Thus, the spin continue to precess with individual frequency, however in the opposite direction. After a time T all spins realign, i.e. they are in phase again (e) and a macroscopic dipole moment forms again. At that time the ensemble of oscillating spins produces an observable signal, i.e. the "echo–signal" (from [8]).

The photon–echo was also observed in the experiment by Brewer and Shoemaker [7] in the following way: Initially the two–level systems were prepared in the coherence plane by using a Stark pulse corresponding to a $\pi/2$–pulse. Then, after waiting for a certain time T a π–pulse was applied which resulted in an echo signal again after waiting for a time T. Detection of the transient signals was done in the same way as for the observation of the optical nutation (see Fig. 18). Note that these striking effects are the result of a collective behavior and are observed with ensembles of atoms. This behavior can be visualized as shown in Fig. 19.

The notion Bloch vector, however, is also used for single atoms and then measurements have to be interpreted in a different way. As we will see later in this lecture (see Chapter 7), it is possible to perform experiments with single atoms and to investigate their dynamical reaction upon the interaction with radiation. Then, the expectation values calculated above (and the experiments of Brewer and

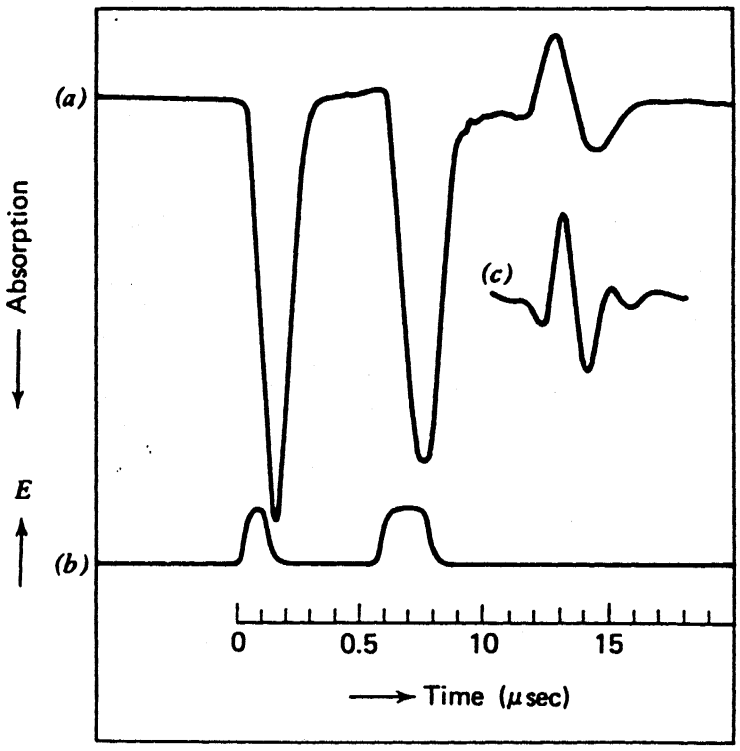

Figure 18: Photon echo observed in CH_3F molecules: (a) observed optical response to the $\pi/2$–pulse (for preparation of the coherence), the π–pulse (for flipping the spins) and the echo signal. (b) Trace of the applied electric field (Stark–pulses). (c) enlarged echo signal for a different electric field switching amplitude (from [7]).

Shoemaker taken from measurements on an ensemble) have to taken from ensembles of individual measurements on a single atom. Thus, the dynamical behavior of the Bloch vector of a single atom can be observed in a similar way. Details of such measurements will be given in Chapter 7 below, Fig. 20 shows Rabi oscillations observed on a single atom.

References

[1] R. Loudon, *The quantum theory of light*, 3rd edition, Oxford Science Publications, Oxford University Press 2000.

[2] C. Cohen-Tannoudji, B. Diu, F. Laloe, *Quantum Mechanics Vol. I, II*, Wiley, New york 1977.

[3] C. W. Gardiner and P. Zoller, *Quantum Noise*, Springer-Verlag, Heidelberg 2000.

[4] R. P. Feynman, F. L. Vernon, and R. W. Hellwarth, J. Appl. Phys. **48**, 49 (1957).

[5] P. Meystre, M. Sargent III; *Elements of Quantum Optics*, Springer–Verlag, Berlin 1990.

[6] H. Haken, *Licht und Materie I*, BI Wissenschaftsverlag, Mannheim 1989.

[7] R. G. Brewer and R. L. Shoemaker, Phys. Rev. Lett. **27**, 631 (1971).

[8] H. Haken, *Light*, Elsevier, Amsterdam 1981.

[9] L. Allen and J.H. Eberly, *Optical Resonance and Two–level atoms*, Dover Publications Inc., New York 1987.

[10] A. Steane, C. F. Roos, D. Stevens, A. Mundt, D. Leibfried, F. Schmidt-Kaler, and R. Blatt, Phys. Rev. **A 62**, 042305 (2000).

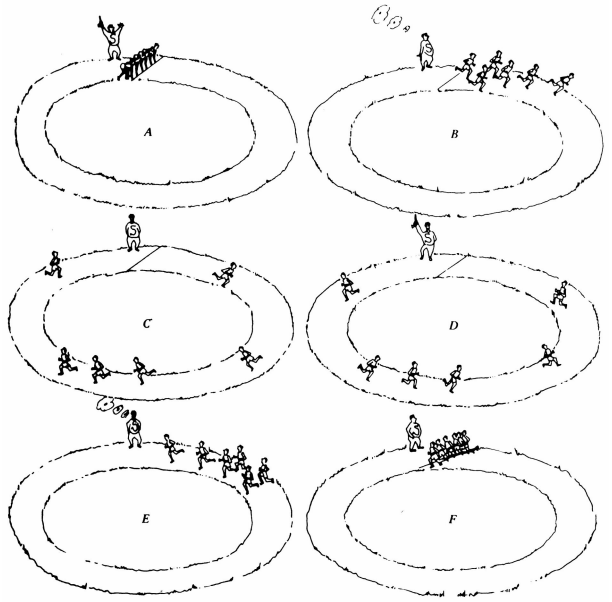

Figure 19: Dephasing, reversal and rephasing of a bulk of runners on a race track, leading to an "echo" of the starting configuration (from [9]).

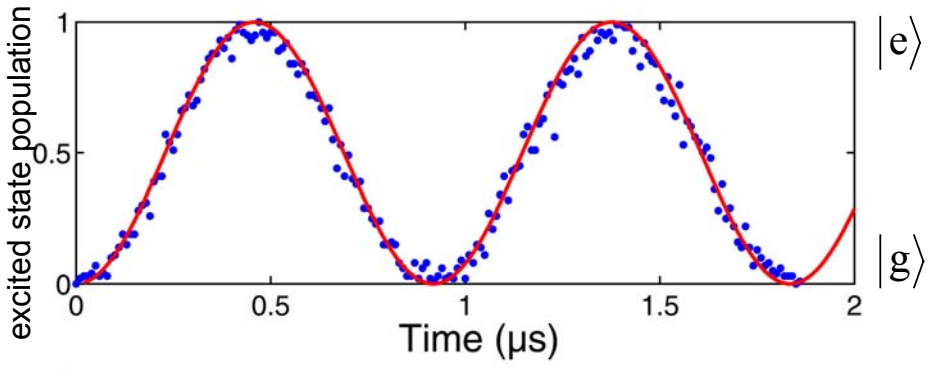

Figure 20: Rabi oscillations observed in a single trapped ion, details of such measurements will be given in Chapter 7 (from [10]).